

Angle-resolved photoemission spectroscopy study of Fe(110) single crystal: Many-body interactions between quasi-particles at the Fermi level

X.Y. Cui^a, K. Shimada^b, M. Hoesch^c, Y. Sakisaka^d, H. Kato^d, Y. Aiura^e,

M. Higashiguchi^a, Y. Miura^a, H. Namatame^b, M. Taniguchi^{a,b}

^aGraduate School of Science, Hiroshima University, Kagamiyama 1-3-1, Higashi-Hiroshima 739-8526, Japan

^bHiroshima Synchrotron Radiation Center, Hiroshima University, Kagamiyama 2-313, Higashi-Hiroshima 739-0046, Japan

^cEuropean Synchrotron Radiation Facility, 6 rue Jules Horowitz BP220, 38043 Grenoble Cedex, France

^dDepartment of Physics, Faculty of Science, Hirosaki University, bunkyo-cho, Hirosaki, Aomori, 036-8560, Japan

^eNational Institute of Advanced Industrial Science and Technology, Tsukuba, Ibaraki 305-8568, Japan

Abstract

A high-resolution angle-resolved photoemission spectroscopy (ARPES) study of Fe(110) single crystal was conducted to elucidate many-body interactions between quasi-particles at the Fermi level at low temperature. Two kink structures were observed in the energy-band dispersion at the binding energies of ~ 40 meV and ~ 270 meV for the bulk-derived band on the majority-spin Fermi surface around the Γ point. Based on analyses of the experimentally obtained real parts of the self-energy, these kink structures are derived from electron-phonon and electron-magnon interactions.

The electronic structure of an itinerant ferromagnet iron has been studied extensively both theoretically [1-3] and experimentally [4-10]. Angle-resolved photoemission spectroscopy (ARPES), which is one of the most powerful methods to directly examine the energy-band and Fermi surface (FS) of solids [11], has already been applied to Fe single crystals [4-9]. Recently, the energy and angular resolution of ARPES has been drastically improved. It is now possible, by means of detailed spectral shape analyses, to estimate the real ($\text{Re}\Sigma$) and imaginary ($\text{Im}\Sigma$) parts of the self-energy, and therefore study the underlying many-body interactions. Schäfer *et al.* examined the surface state of Fe(110) thin film grown on W(110) using high-resolution ARPES, and evaluated $\text{Re}\Sigma$ and $\text{Im}\Sigma$ [7]. They found electronic states are coupled to a bosonic mode with a characteristic cut-off energy at ~ 160 meV in the density-of-

states (DOS). On the basis of the inelastic neutron scattering results [10], it was claimed that the bosonic mode should be magnon. Furthermore, they undertook extensive FS mapping and concluded that the experimental Fermi velocities were much smaller than those given by the band-structure calculation [8]. This implies that strong renormalization exists near the Fermi level (E_F) [8].

In order to elucidate many-body interactions between quasi-particles in the bulk-derived electronic states quantitatively, we carried out a high-resolution ARPES study using Fe(110) single crystal at low temperature, and examined in detail the majority-spin band on a FS surrounding the Γ point. We found two kink structures in the energy-band dispersion. The real part of the self-energy was experimentally determined. On the basis of the analyses of $\text{Re}\Sigma$, these two kink structures originate from the electron-phonon and electron-magnon

interactions.

The Fe(110) single crystal sample was cleaned by Ar⁺ ion sputtering and subsequent annealing at 570°C for 30 minutes.[6,9] Cleanliness of the sample surface was checked by Auger electron spectroscopy and ultraviolet photoemission spectra. Impurities such as carbon, nitrogen, oxygen and sulfur were below the detection limit. The high-resolution ARPES measurements were carried out at the linear undulator beamline BL-1 on a compact electron-storage ring (HiSOR) at the Hiroshima Synchrotron Radiation Center (HSRC), Hiroshima University [12]. The hemispherical electron-energy analyzer (ESCA200, SCIENTA), operating in multi-channel angular mode, was used for ARPES measurements. Angular and energy resolutions were set respectively at $\Delta\theta = 0.3^\circ$ ($\Delta k = 0.016 \text{ \AA}^{-1}$) and 9 meV at the photon energy of $h\nu = 40$ eV. The single crystal sample was mounted on a low-temperature goniometer (R-Dec Co. Ltd., i-GONIO LT) and cooled to 15 K. The pressure of the main chamber was better than 1×10^{-10} Torr. The parallel and perpendicular components of the photoelectron wave vectors relative to the surface, k_{\parallel} and k_{\perp} , were determined by the equations $k_{\parallel} = \sqrt{2mE_k / h^2 \sin \theta}$ and $k_{\perp} = \sqrt{(2m/h^2)(E_k \cos^2 \theta + V_0)}$, where E_k is the kinetic energy of the photoelectron, V_0 is the inner potential. Here we assumed $V_0 = 14.3$ eV [8].

Figure 1 shows the majority-spin (thick lines) and minority-spin (thin lines) FSs around the Γ point, calculated by the band-structure calculation [13], for the parts of the FSs covered by this study. The electron-energy-analyzer slit and the [1̄12] direction of the sample were parallel. The polar angle of the ARPES measurements was set parallel to the [̄111] direction. We varied the polar angle and observed the majority-spin band crossing E_F . We selected the incident photon energy of $h\nu = 40$ eV, at which one can see a majority-spin band crossing E_F at a k point indicated in a grey circle in

Fig. 1. This band is most suitable since the peak has a narrow width and a parabolic dispersion. Furthermore, the background interference is minimal.

Figure 2(a) shows the obtained intensity plot of the majority-spin band crossing E_F . Figures 2(b) and 2(c) show energy distribution curves (EDCs) and a momentum distribution curve (MDC) at E_F , respectively. As the peak approaches E_F , the peak becomes stronger and narrower. As the peak binding energy increases, especially for $E_B > \sim 400$ meV, the peak broadens rapidly.

We determined the band points by fitting a MDC for each binding energy with a Lorentzian on a linear background as shown in Fig. 3(a). The group velocity, $v_F = (1/h)(dE/dk)$, decreases below $E_B \sim 270$ meV; One can recognize a ‘kink’, or a sudden change of v_F , below $E_B \sim 270$ meV. The energy of the kink coincides well with the cut-off energy of the calculated magnon DOS [14]. Since the cut-off energy in the magnon DOS is determined by the optic mode, the correlation with the optic mode cannot be ignored. We should also note that we cannot see clearly an anomaly in the present bulk-derived band at $E_B \sim 160$ meV as seen in the surface state of Fe [8].

Figure 3(b) exhibits observed energy-band dispersion near E_F . One can also recognize a kink around $E_B \sim 40$ meV. Since the Debye temperature of Fe is $\Theta_D = 470$ K ($k_B \Theta_D = 40$ meV), it is reasonable to assume that the spectral features at $E_B \sim 40$ meV are derived from the electron-phonon interaction [9]. We should also note that the cut-off energy of the calculated phonon DOS [15] coincides well with the energy scale of the observed kink structure.

In order to elucidate many-body interactions in more detail, we evaluated the real part of the self-energy. ARPES spectrum measures the quasi-particle spectral function [11,16,17]:

$$A(k,\omega) = -\frac{1}{\pi} \frac{\text{Im}\Sigma(k,\omega)}{[\omega - \varepsilon_k - \text{Re}\Sigma(k,\omega)]^2 + [\text{Im}\Sigma(k,\omega)]^2}. \quad (1)$$

One can evaluate $2|\text{Im}\Sigma|$ and $\text{Re}\Sigma$ experimentally by the spectral width ($\Gamma = \delta E = 2|\text{Im}\Sigma|$) and the energy shift from the non-interacting band, ε_k^0 : $\text{Re}\Sigma = \varepsilon_k - \varepsilon_k^0$, where ε_k is the observed energy for the band points [11,16,17]. In the present case, we assumed that the non-interacting energy-band dispersion is given by $\varepsilon_0(k) = -a(k-k_F) + b(k-k_F)^2$. We found that $a = 2.63 \text{ eV}\cdot\text{\AA}$ and $b = 1.63 \text{ eV}\cdot\text{\AA}^2$ reproduce the experimental group velocity for $E_B > \sim 350 \text{ meV}$. The resulting $\text{Re}\Sigma$ is shown in Fig. 3(c). One can see the observed $\text{Re}\Sigma$ exhibit two peak features at $E_B \sim 40 \text{ meV}$ and $\sim 270 \text{ meV}$. This indicates that there exist two different energy scales derived from many-body interactions.

Here we assumed that the lifetime broadening of ARPES spectra (Γ_{total}) can be expressed by the sum of independent interactions: $\Gamma_{\text{total}} = \Gamma_{\text{el-ph}} + \Gamma_{\text{el-el}} + \Gamma_{\text{el-mag}} + \Gamma_0$, where $\Gamma_{\text{el-ph}}$, $\Gamma_{\text{el-mag}}$ and $\Gamma_{\text{el-el}}$ are the lifetime broadening due to the electron-phonon, electron-magnon, and electron-electron, respectively [17]. Γ_0 represents the energy independent term mainly derived from the final-state broadening [17]. Since the energy scale of the electron-electron interaction is expected to be the bandwidth of Fe 3d states, $\sim 5 \text{ eV}$, it is much larger compared to those of the electron-phonon and electron-magnon interactions. The real part of the self-energy due to electron-electron interaction should not yield fine spectral structures in the energy range we examined. Therefore we will consider $\text{Re}\Sigma$ derived from the electron-phonon and electron-magnon interactions in the present analyses.

The lifetime broadening due to $\Gamma_{\text{el-ph}}$ is given by

$$\Gamma_{\text{el-ph}} = 2\pi \int_0^\infty \alpha^2 F(v) [2n(v,T) + f(v+\omega,T) + f(v-\omega,T)] dv \quad (2)$$

where $n(v,T)$ and $f(v,T)$ are Bose-Einstein, and Fermi-Dirac

distribution functions, respectively [16,17]. The function $\alpha^2 F(v)$ is the Eliashberg function, and we assumed that α is an adjustable parameter multiplied by the calculated phonon DOS, $F(v)$ [15]. We also assumed (2) for the lifetime broadening of the electron-magnon interaction ($\Gamma_{\text{el-mag}}$). Here we calculated $\Gamma_{\text{el-mag}}$ using the magnon DOS given by band-structure calculation [14]. $\text{Re}\Sigma$ values are calculated to satisfy the Kramers-Kronig relation with respect to $|\text{Im}\Sigma| = \Gamma/2$ [17].

The calculated $\text{Re}\Sigma$ s derived from the electron-phonon and electron-magnon interactions are shown in Fig. 3(c). One can clearly see that the peak at $\sim 40 \text{ meV}$ and $\sim 270 \text{ meV}$ in the observed $\text{Re}\Sigma$ closely correlate with the calculated ones. This confirms that the kink structures at $\sim 40 \text{ meV}$ and $\sim 270 \text{ meV}$ originate from the electron-phonon and electron-magnon interactions, respectively.

The strength of a many-body interaction is measured by the coupling constant; $\lambda = |\partial \text{Re}\Sigma / \partial \omega|_{\omega=0}$. We obtained $\lambda = 0.07 \pm 0.01$ and 0.14 ± 0.03 for electron-phonon and electron-magnon interactions, respectively. The strength of the coupling constant of the electron-magnon interaction is larger than that of the electron-phonon interaction.

In summary, we performed high-resolution ARPES measurements on a Fe(110) bulk single crystal at low temperature. We examined a bulk-derived majority-spin band on a FS surrounding the Γ point and found two kink structures at $\sim 40 \text{ meV}$ and $\sim 270 \text{ meV}$ in the energy-band dispersion. On the basis of the analyses of $\text{Re}\Sigma$, the former is derived from the electron-phonon interaction and the latter from the electron-magnon interaction. For the band we examined, the contribution of the electron-magnon interaction to the quasi-particle effective mass enhancement is more significant than that of the electron-phonon interaction.

This work was partly supported by a Grant-in-Aid for Scientific Research (No. 17654060) by MEXT of Japan. We

thank the N-BARD, Hiroshima University for supplying liquid helium. The synchrotron radiation experiments were carried out with the approval of HSRC (Proposal No. 04-A-58).

References

- [1] J. Callaway and C.S. Wang, Phys. Rev. B **16** (1977) 2095.
- [2] J. Callaway and C.S. Wang, Phys. Rev. B **53** (1984) 612.
- [3] J. Redinger *et al.*, Phys. Rev. B **38**, 5203 (1988).
- [4] D. E. Eastman *et al.*, Phys. Rev. Lett. **44**, 95 (1980).
- [5] A.M. Turner, and J.L. Erskine, Phys. Rev. B **30**, 6675 (1984).
- [6] Y. Sakisaka *et al.*, Phys. Rev. **41** (1990) 11865.
- [7] J. Schäfer *et al.*, Phys. Rev. Lett. **92** (2004) 097205.
- [8] J. Schäfer *et al.*, Phys. Rev. B **72** (2005) 155115.
- [9] X.Y. Cui *et al.*, Physica B. **383** (2006) 146.
- [10] D. McKenzie Paul *et al.*, Phys. Rev. B **38**, 580 (1988).
- [11] S. Hüfner, *Photoelectron Spectroscopy 3rd ed.* (Springer-Verlag, Berlin, 2003).
- [12] K. Shimada *et al.*, Surf. Rev. Lett. **9** (2002) 529.
- [13] P. Blaha, K. Schwarz, G.K. H. Madsen, D. Kvasnicka, and J. Luitz, /WIEN2K/ (Technical University of Vienna, Austria, 2001).
- [14] S.V. Halilov *et al.*, Phys. Rev. B **58** (1998) 293.
- [15] M. Seto *et al.*, Phys. Rev. Lett. **74** (1995) 3128.
- [16] T. Valla *et al.*, Phys. Rev. Lett. **83** (1999) 2085.
- [17] M. Higashiguchi *et al.*, Phys. Rev. B **72** (2005) 214438.

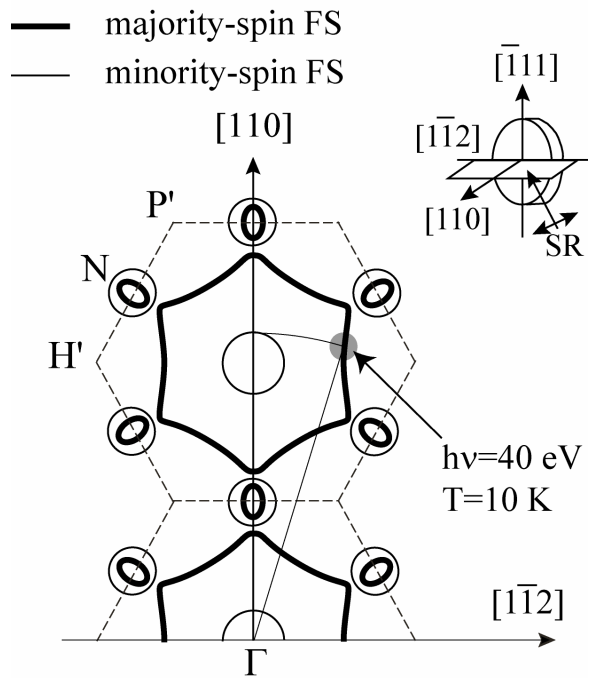


Fig. 1

Measured portion of the FSs in the present study together with the calculated cross-section of the majority-spin (thick lines) and minority-spin (thin lines) FSs [13].

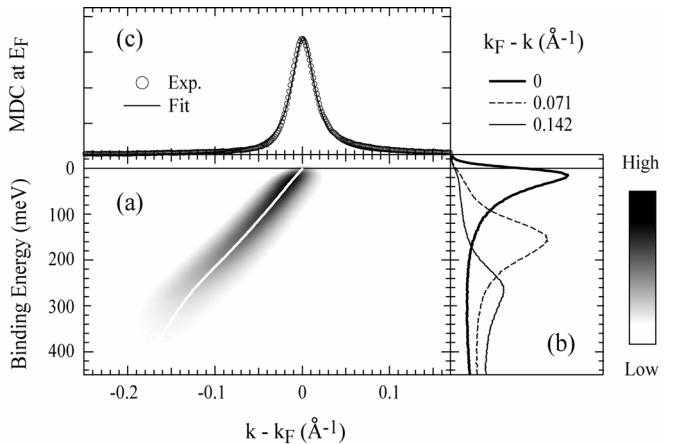


Fig. 2

ARPES results of Fe(110) taken at $h\nu = 40$ eV at 15 K. (a) Intensity plot. White line indicates evaluated peak locations. (b) EDCs as a function of $k_F - k$. (c) MDC near E_F . The solid line shows a fitted curve.

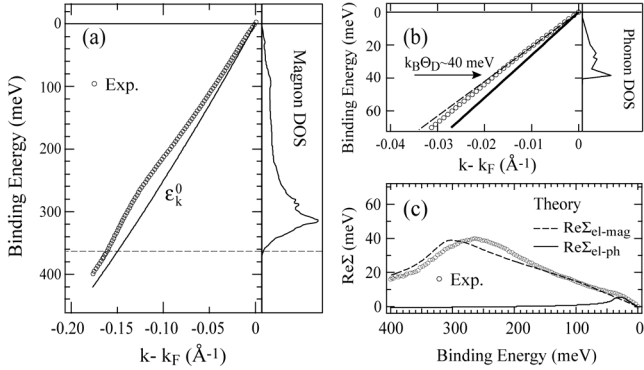


Fig.3

(a) Experimentally determined band points (open circles) determined from the MDCs taken at $h\nu = 40$ eV. The solid line indicates the assumed non-interacting band, ε_k^0 . The magnon DOS of bcc Fe [14] is also shown. (b) Experimental band dispersion near E_F . Dashed and solid lines represent the gradient of the energy-band dispersion at E_F and ε_k^0 , respectively. Calculated phonon DOS [15] is also shown. (c) Observed $\text{Re}\Sigma$ compared with calculated $\text{Re}\Sigma_{\text{el-mag}}$ and $\text{Re}\Sigma_{\text{el-ph}}$.